Electronic Supplementary Material (ESI) for Dalton Transactions.

Supporting Information

A NbO type Cu(II) metal–organic framework showing efficient catalytic activity in Friedländer and Henry reactions

*Anoop K. Gupta, Dinesh De, Parimal K. Bharadwaj**

Department of Chemistry, Indian Institute of Technology Kanpur, UP-208016, India.

Materials and Physical Measurements

Materials

Reagent grade chemicals 5-aminoisophthalic acid, 1,2-dibromo-ethane (98%), and $Cu(NO_3)_2 \cdot 3H_2O$ (99%) were obtained from Sigma-Aldrich and used as received except to 1,2-dibromo-ethane. 1,2-dibromo-ethane and other chemicals and solvents that were procured from S. D. Fine Chemicals (India), were freshly purified prior to use.

Physical Measurements

Infrared spectra were recorded on Perkin-Elmer Model 1320 spectrometer (KBr disk, 400–4000 cm^{-1}). ^1H NMR and ^{13}C NMR spectra were recorded on a JEOL-ECX 500 FT (500 MHz and 125 MHz respectively) instrument in$CDCl_3$ and DMSO-d_6 with Me_4Si as the internal standard or on a JEOL ECS 400 FT (400, 100 MHz respectively) instrument in $CDCl_3$ or in DMSO-d_6 with Me4Si as the internal standard. ESI-mass spectra were recorded on a WATERS Q-TOF Premier mass spectrometer. Thermogravimetric analyses (TGA) were performed on Mettler Toledo Star System (heating rate of 5°C/min). Microanalyses for the compounds were obtained using a CE-440 elemental analyzer (Exeter Analytical Inc.). Powder X-ray diffraction (PXRD) patterns were recorded with a Bruker D8 Advance diffractometer equipped with nickel-filtered Cu Kα radiation. The tube voltage and current were 40 kV and 40 mA, respectively.

Synthetic Methodology.

The synthesis of the previously reported linker was achieved by following the reported methods[1] as illustrated in Scheme S1.

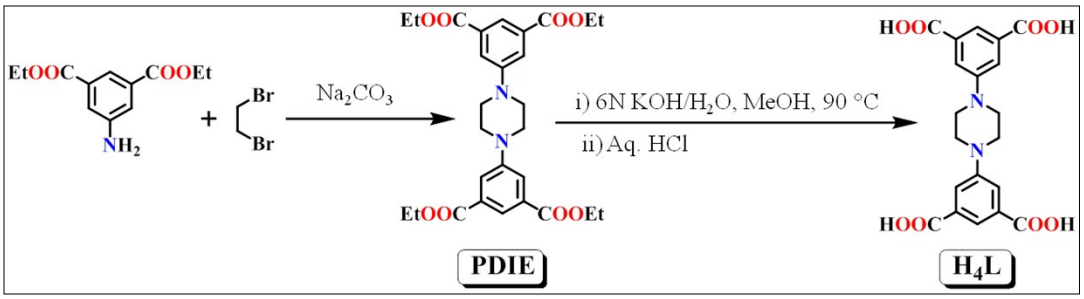

Scheme S1 Synthesis of **H_4L** Ligand.

Synthesis of tetraethyl 5,5'-(piperazine-1,4-diyl)diisophthalate, (PDIE):

A mixture of 5-aminoisophthalate-diethyl ester[2] (10 g, 42.2 mmol), anhydrous Na_2CO_3 (2.73 g, 10.00 mmol) in toluene (40 mL) was combined with cesium carbonate (20 g, 200 mmol), and freshly purified 1,2-dibromo-ethane (45 mL, 528 mmol) were added in a 250 ml two neck flask under N_2 atmosphere. The mixture was stirred at 90 °C for 12 h then 130 °C for next 12 h and finally at 160 °C for 24 h. After this the reaction mixture was poured in beaker and evaporated in hood by continuous blow of hot air. Water (150 mL) and $CHCl_3$ was added to the reaction mixture. The aqueous phase was extracted three times with $CHCl_3$. The combined organic phases were passed through anhydrous sodium sulfate and evaporated to dryness to obtain the crude product as a light yellow solid. It was purified by column chromatography using silica gel (200 mesh). Elution with 20% ethyl acetate in *n*-hexane gave tetraethyl 5,5'-(piperazine-1,4-diyl)diisophthalate, (PDIE) as a pale yellow crystalline powder (6.1 g, yield: 27.5% based on 5-aminoisophthalate-diethyl ester). FT–IR (KBr, cm^{-1}): 3415 (broad), 2985 (m), 1718 (s), 1602 (m), 1456 (m), 1375 (s), 1351 (m), 1238 (s), 1141 (s), 1064 (m), 999 (s), 868 (m), 756 (s), 682 (m); ^1H NMR (500 MHz, $CDCl_3$, 25 °C, $Si(CH_3)_4$): δ (ppm) = 8.17 (s, 2H, Ar–H), 7.81 (s, 4H, Ar–H), 4.40 (q, J= 7.45 Hz, 8H, $–OCH_2$) 3.46 (s, 8H, $–CH_2–$), 1.41 (t, J= 7.45 Hz, 12H, $–CH_3$); ^{13}C NMR (125 MHz, $CDCl_3$, 25 °C, $Si(CH_3)_4$): δ (ppm) = 14.43, 48.80, 61.42, 120.91, 121.82,

131.86, 151.07, 166.24; ESI-MS: (m/z): 527.2393 (100%) $[M+H]^+$; anal. calcd (%) for $C_{28}H_{34}N_2O_8$ (M = 526.58): C, 63.86; H, 6.51; N, 5.32. Found: C, 63.42; H, 6.68; N, 5.54.

Synthesis of 5,5'-(piperazine-1,4-diyl)diisophthalic acid, (H_4L):

Tetraester PDIE (5 g, 1.03 mmol) was suspended in methanol (250 mL) and water (180 mL). After adding KOH (20 g, 3.75 mmol), the reaction mixture was refluxed for overnight. Then most of the solvent was evaporated *in vacuo*. After removal solvent, water was added to fully dissolve the precipitate. The aqueous solution was acidified with concentrated HCl to pH~5. The light yellow precipitate formed was collected by filtration, washed with water, and dried at room temperature to obtain **H_4L** (3.6 g, yield: 91.4%). M.P.: >300°C; FT–IR (KBr, cm^{-1}): 3345 (s), 3089 (m), 2844 (m), 1731 (s), 1674 (s), 1603 (s), 1464 (s), 1422 (s), 1385 (m), 1269 (s), 1191 (s), 1149 (s), 1061 (m), 998 (s), 881 (m), 786 (s), 668 (s); ^{1}H NMR (500 MHz, DMSO–d^6, 25 °C, $Si(CH_3)_4$): δ (ppm) = 13.10 (broad, 4H, –COOH), 7.90 (s, 2H, Ar–H), 7.69 (s, 4H, Ar–H), 3.38 (s, 8H, $–CH_2–$); ^{13}C NMR (125 MHz, DMSO–d^6, 25 °C, $Si(CH_3)_4$): δ (ppm) = 48.27, 120.11, 120.97, 132.60, 151.47, 167.49; ESI−MS: (m/z): 413.0984 (100%) $[M−H]^–$; anal. calcd (%) for $C_{20}H_{18}N_2O_8$ (M = 414.37): C, 57.97; H, 4.38; N, 6.76. Found: C, 57.21; H, 4.53; N, 6.89.

X-ray Structural Studies

The crystal data for the **1** has been collected on a Bruker *SMART* CCD diffractometer (Mo Kα radiation, λ = 0.71073 Å). The program *SMART*[3] was used for collecting frames of data, indexing reflections, and determining lattice parameters; *SAINT*[3] for integration of the intensity of reflections and scaling; *SADABS*[4] for absorption correction; and *SHELXTL*[5] for space group and structure determination and least-squares refinements on F^2. The crystal structures were solved and refined by full-matrix least-squares methods against F^2 by using the program *SHELXL-2014*[6] using *Olex-2* software.[7] All the non-hydrogen atoms were refined with

anisotropic displacement parameters. Hydrogen positions were fixed at calculated positions and refined isotropically. The unit cell includes large region of disordered solvent molecules which could not be modeled as discrete atomic sites. We employed PLATON/SQUEEZE[8] to calculate the diffraction contribution of solvent molecules. In spite of our best efforts to obtain the best quality data, the structure generates some alerts in check CIFs whose plausible origins are due to flexible nature of piperazine part in the ligand. Crystallographic data have been deposited with the Cambridge Crystallographic Data Center and CCDC number: 1542257. Lattice parameters of the **1**, data collection and refinement parameters are summarized in Table S1 and selected bond distances and bond angles are given in Table S2.

General Procedure for the Friedländer Reaction.

In a typical experiment, 2-aminoketone (0.5 mmol), active methylene compound (5 mmol for ethyl acetoacetate and acetylacetone, and 1 mmol for cyclohexane-1,3-dione with 0.5 mL chloroform) and active catalyst **1′** (5 wt %) were mixed in sealed tube. The reaction tube were filled with nitrogen. The reaction mixture were stirred at 85 ºC for 24 h and the progress of the reaction was monitored by the TLC analysis (1:2 v/v EtOAc/n-hexane as eluent). After completion of the reaction, the reaction mixture was filtered and washed with chloroform. The purification of the reaction mixture was occurred by silica gel column chromatography.

General Procedure for the Henry Reaction.

To a solution of nitroalkane (10 mmol) and aromatic aldehyde (0.5 mmol), the active catalyst **1′** (5 wt %) was added. The reaction mixture was heated at 50 ºC for 48 h with continuous stirring. The reaction progress was monitored by TLC (1:4 v/v EtOAc/n-hexane as eluent). When the

reaction was over, the reaction mixture was filtered and subsequently washed with ethyl acetate and acetone. The filtrate was evaporated at room temperature. The crude product was purified by silica gel column chromatography using petroleum ether and ethyl acetate as eluent followed by evaporation at room temperature.

Table S1. Crystal and Structure Refinement Data for (**1**).

Parameters	**1**
Empirical formula	$C_{14.5}$ $H_{23.5}$ Cu $N_{2.5}$ $O_{8.5}$
Formula wt	432.39
Crystal system	trigonal
Space group	*R*–3m
a, Å	18.604(5)
b, Å	18.604(5)
c, Å	37.123(5)
α (deg)	90
β (deg)	90
γ (deg)	120
V, Å^3	11127(6)
Z	18
ρ_{calc} g/cm^3	0.765
μ, mm^{-1}	0.887
Temperature (ºK)	100(2)
θ max	25.499

F(000)	2574
Refl. collected	41802
Independent refl.	2543
GOOF	1.060
Final R indices [I > 2σ(I)]	R1 = 0.0915 WR2 = 0.2509
R indices (all data)	R1 = 0.1557 WR2 = 0.2959

Table S2. Bond distances and angles.

{[Cu_2(L)(H_2O)$_2$]·(3DMF)(4H_2O)}$_n$ (1)					
Bond Distances (Å)					
Cu1−Cu1^1	2.641(2)	Cu1−O2^2	1.927(5)	Cu1−O3^2	1.952(5)
Cu1−OW1	2.159(7)				
Bond Angles (°)					
O2−Cu1−Cu1^1	85.23(14)	O2^2−Cu1−O2	88.4(3)	O2−Cu1−O3	90.2(2)
O2^2−Cu1−O3	168.25(19)	O2^2−Cu1−OW1	98.8(2)	O3^2−Cu1−Cu1^1	83.03(14)
O3−Cu1−O3^2	88.7(3)	O3−Cu1−OW1	93.0(2)	OW1−Cu1−Cu1^1	174.4(2)

Symmetry Code: (1) -x,1-y,-z; (2) +x,1+x-y,+z;

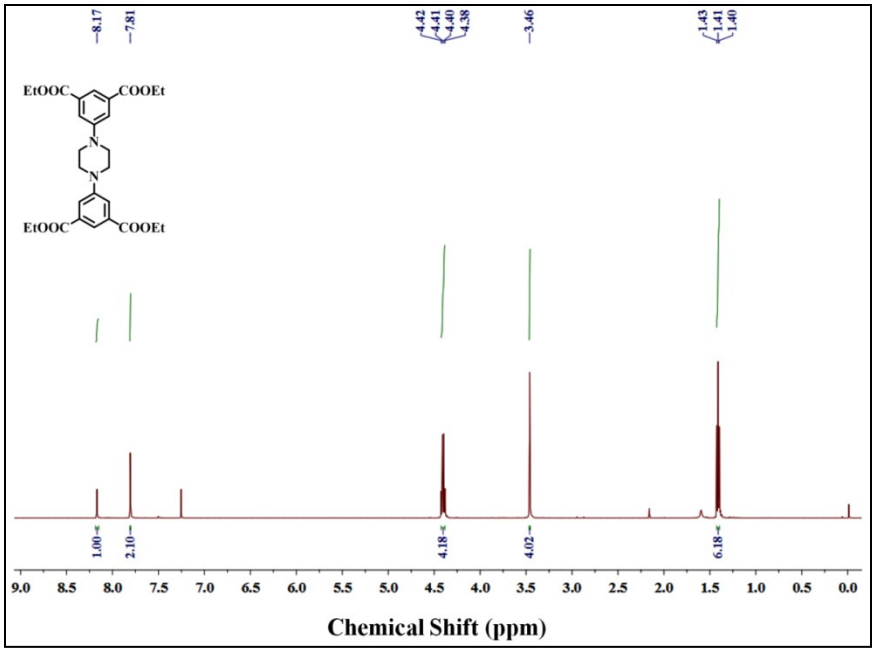

Fig. S1 The ^{1}H NMR spectrum of PDIE.

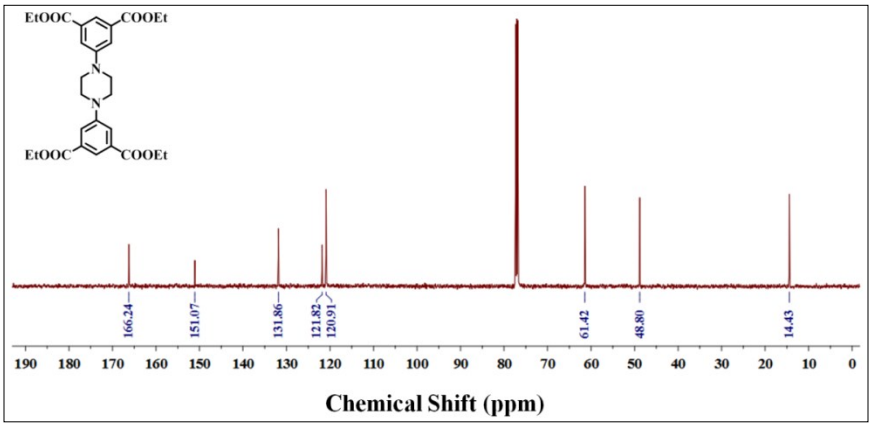

Fig. S2 The ^{13}C NMR spectrum of PDIE.

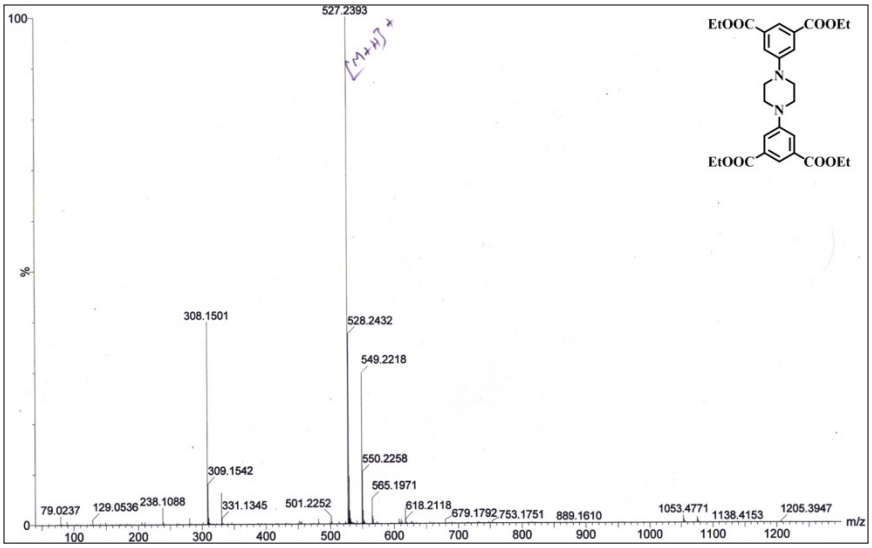

Fig. S3 ESI−MS of PDIE.

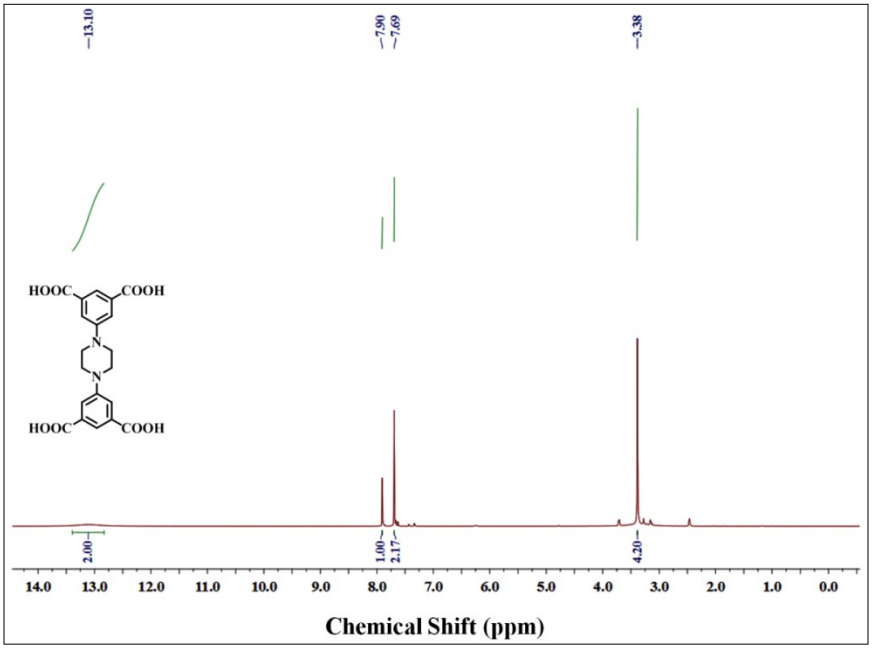

Fig. S4 The ^{1}H NMR spectrum of $\mathbf{H_4L}$.

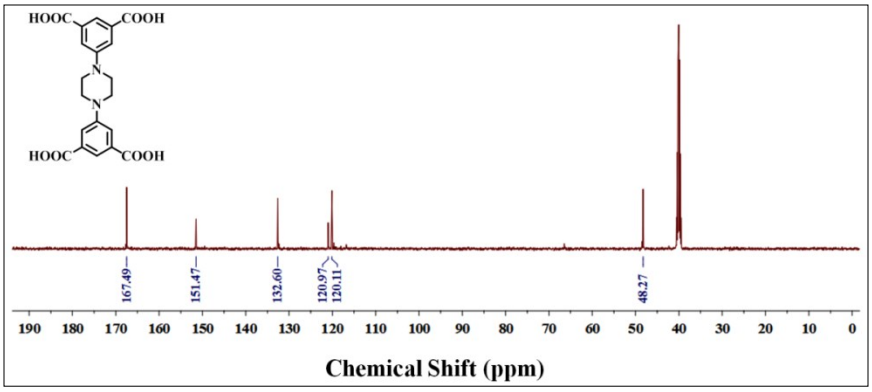

Fig. S5 The ^{13}C NMR spectrum of $\mathbf{H_4L}$.

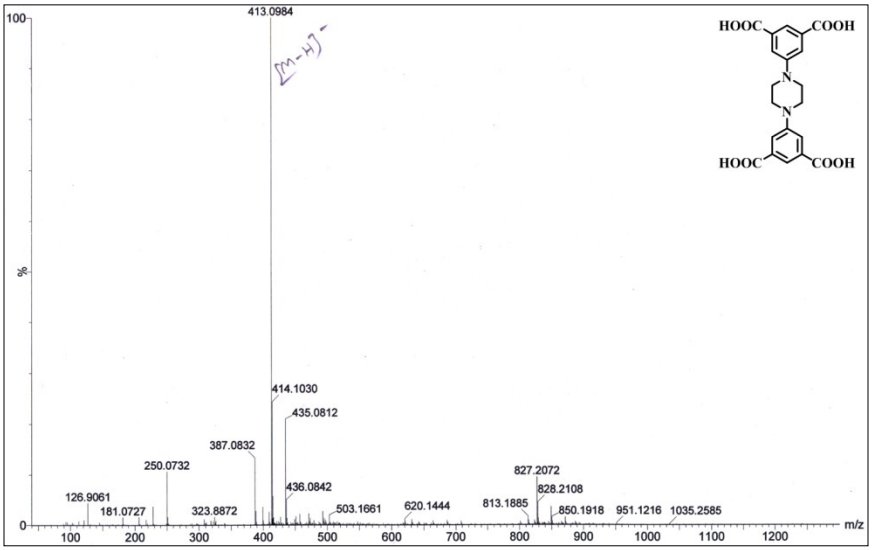

Fig. S6 ESI−MS of $\mathbf{H_4L}$.

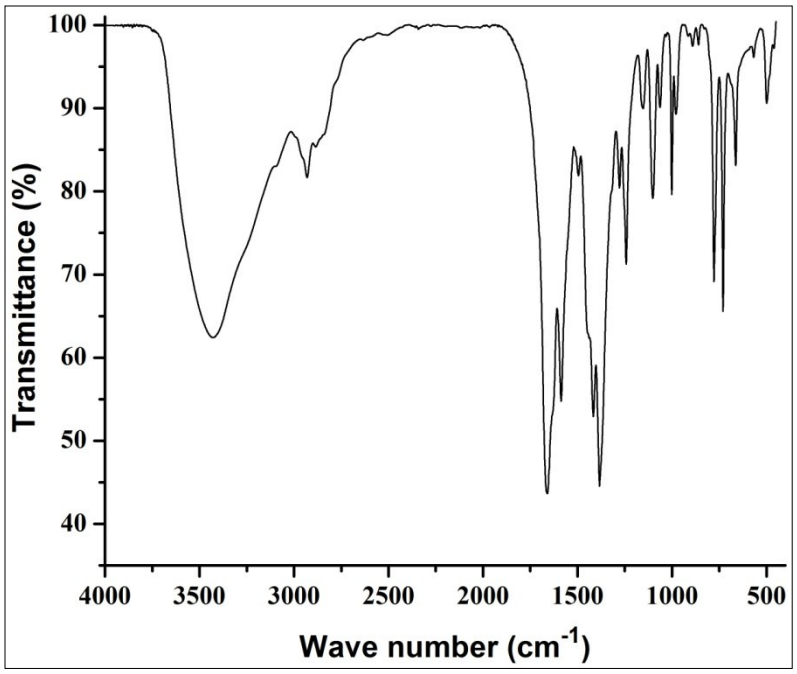

Fig. S7 FT−IR spectrum of **1**.

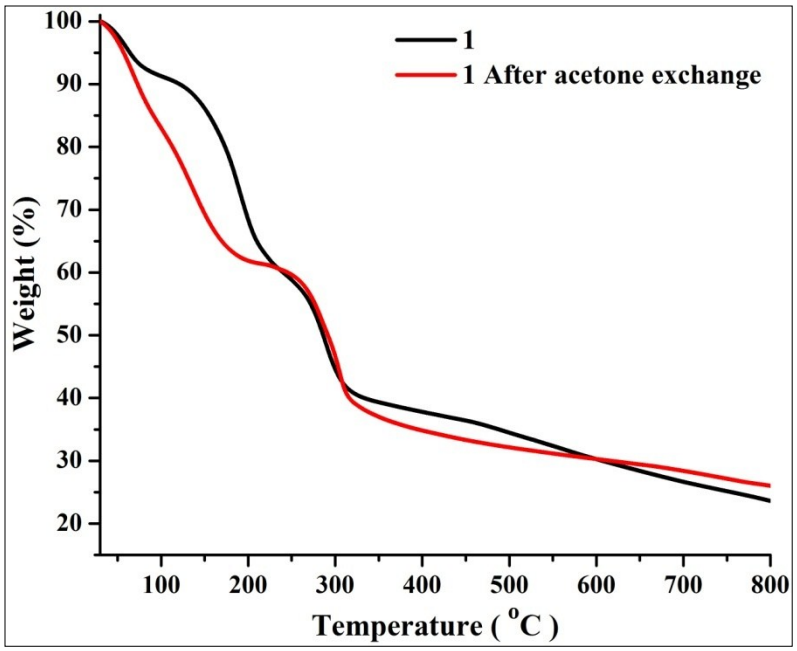

Fig. S8 Thermogravimetric analysis curve of **1**: as synthesized (black color) and after acetone exchange (red color).

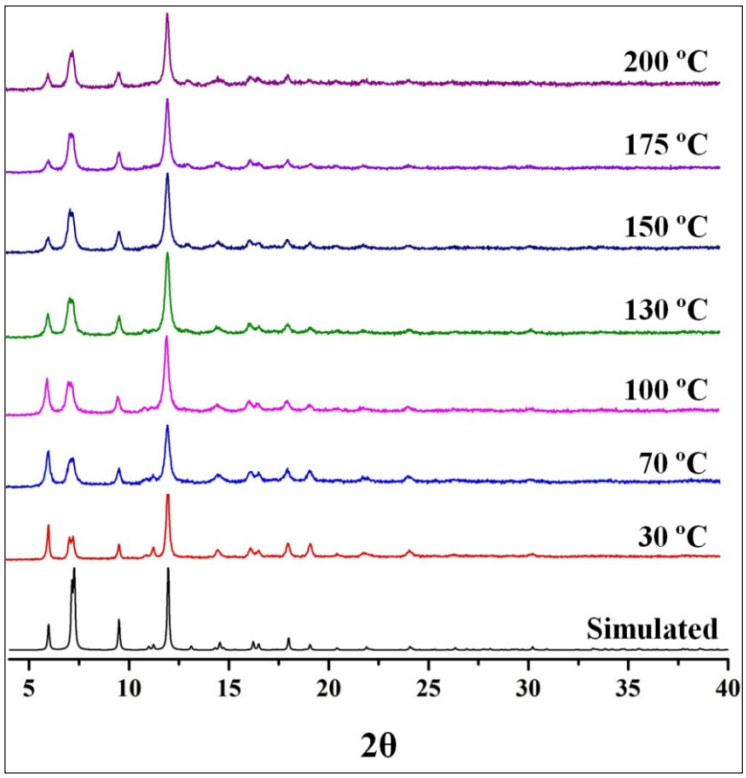

Fig. S9 Variable temperature powder X-ray diffraction patterns of **1**.

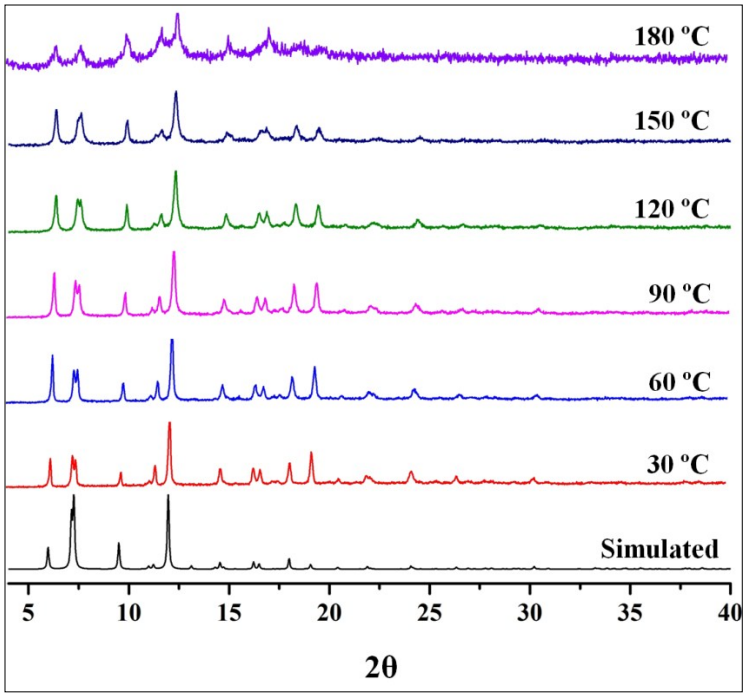

Fig. S10 Variable temperature powder X-ray diffraction patterns of **1** after acetone exchange.

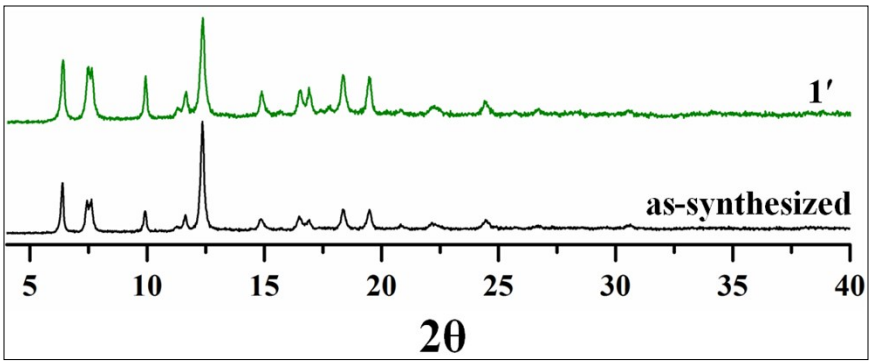

Fig. S11 Powder X-ray diffraction patterns of as-synthesized and activated sample.

Compounds Characterization Data for Friedländer Reactions

Ethyl-2-methyl-4-phenylquinoline-3-carboxylate (Table1, entry 1). ^{1}H NMR (400 MHz, CDCl3): δ (ppm) 8.04 (d, J = 8.24 Hz, 1H, Ar–H), 7.67 (t, J = 8.24 Hz, 1H, Ar–H), 7.54 (d, J = 7.36 Hz, 1H, Ar–H), 7.43–7.46 (m, 3H, Ar–H), 7.34–7.39 (m, 1H, Ar–H), 7.32–7.33 (m, 2H, Ar–H), 4.03 (q, J = 7.36 Hz, 2H, –OCH_2), 2.76 (s, 3H, –CH_3), 0.91 (t, J = 6.88 Hz, 3H, –CH_3); ^{13}C NMR (100 MHz, $CDCl_3$) δ = (ppm) 13.71, 23.90, 61.40, 125.20, 126.49, 126.56, 127.47, 128.30, 128.53, 128.92, 129.44, 130.33, 135.80, 146.32, 147.77, 154.67, 168.53; MS (ESI): m/z = 292.13 $[M+H]^+$.

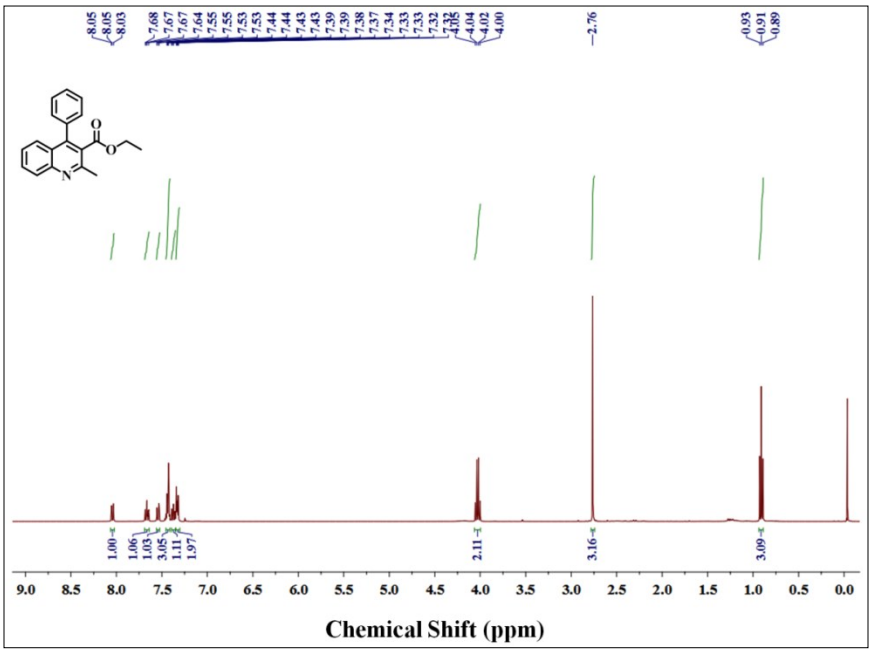

Fig. S12 ^{1}H NMR of ethyl-2-methyl-4-phenylquinoline-3-carboxylate.

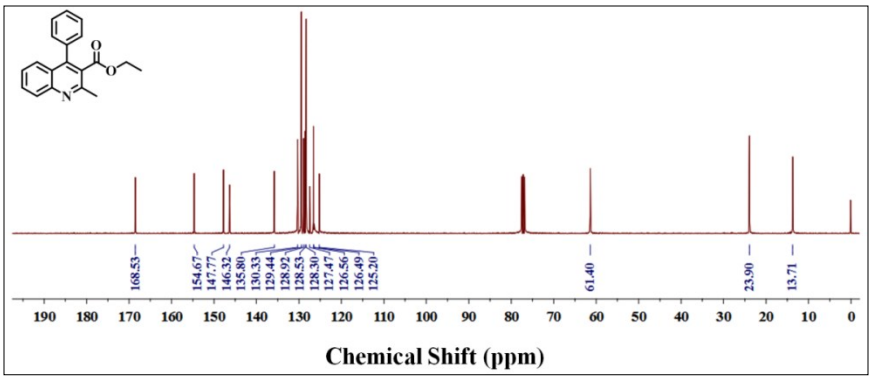

Fig. S13 ^{13}C NMR of ethyl-2-methyl-4-phenylquinoline-3-carboxylate.

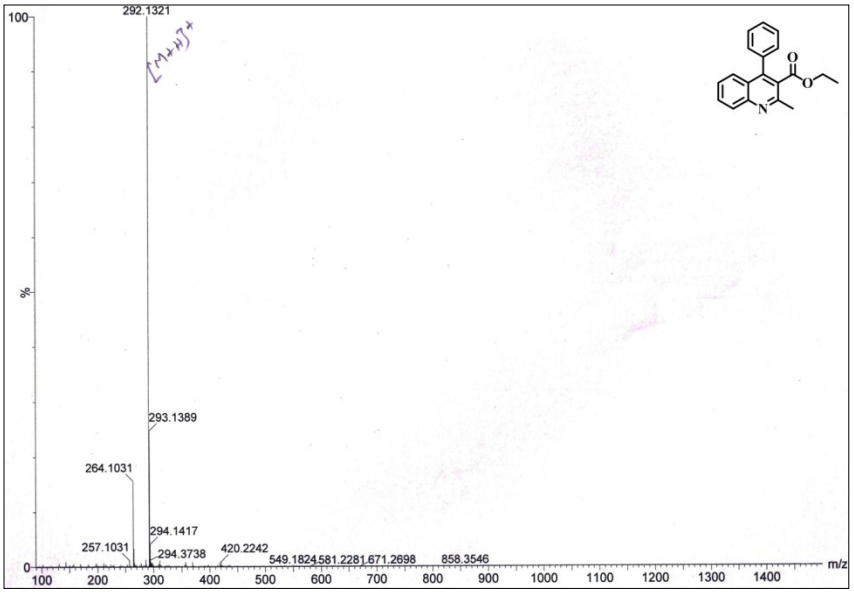

Fig. S14 ESI−MS of ethyl-2-methyl-4-phenylquinoline-3-carboxylate.

Ethyl 6-chloro-2-methyl-4-phenylquinoline-3-carboxylate (Table1, entry 2). ^{1}H NMR (400 MHz, CDCl3): δ (ppm) 7.96 (d, J = 8.72 Hz, 1H, Ar–H), 7.59 (d, J = 9.16 Hz, 1H, Ar–H), 7.44–7.50 (m, 4H, Ar–H), 7.29–7.32 (m, 2H, Ar–H), 4.03 (q, J = 7.32 Hz, 2H, –OCH_2), 2.73 (s, 3H, –CH_3), 0.90 (t, J = 7.32 Hz, 3H, –CH_3); ^{13}C NMR (100 MHz, $CDCl_3$) δ = (ppm) 13.70, 23.82, 61.54, 125.26, 126.00, 128.23, 128.52, 128.84, 129.35, 130.58, 131.18, 132.39, 135.07, 145.45, 146.12, 155.06, 168.15; MS (ESI): m/z = 326.27 $[M+H]^+$.

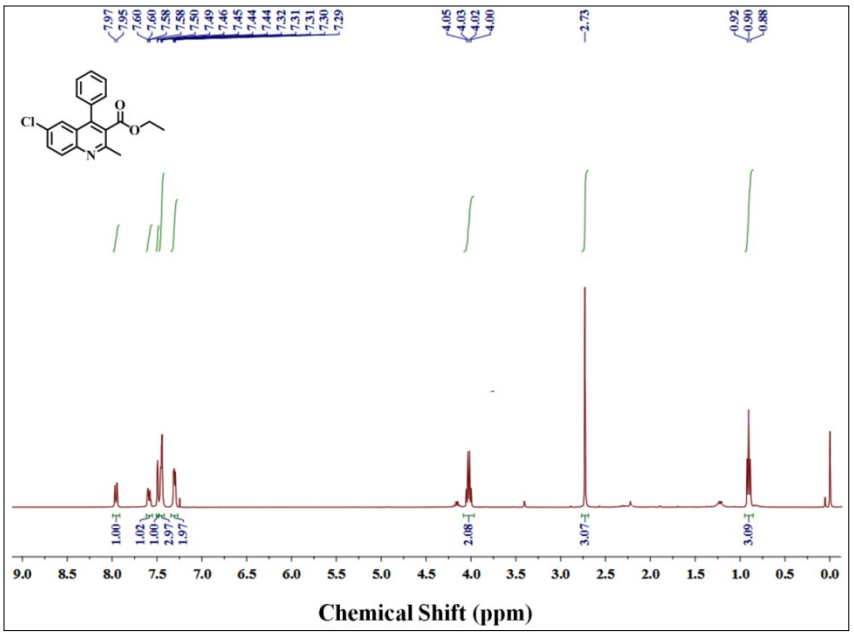

Fig. S15 ^{1}H NMR of Ethyl 6-chloro-2-methyl-4-phenylquinoline-3-carboxylate.

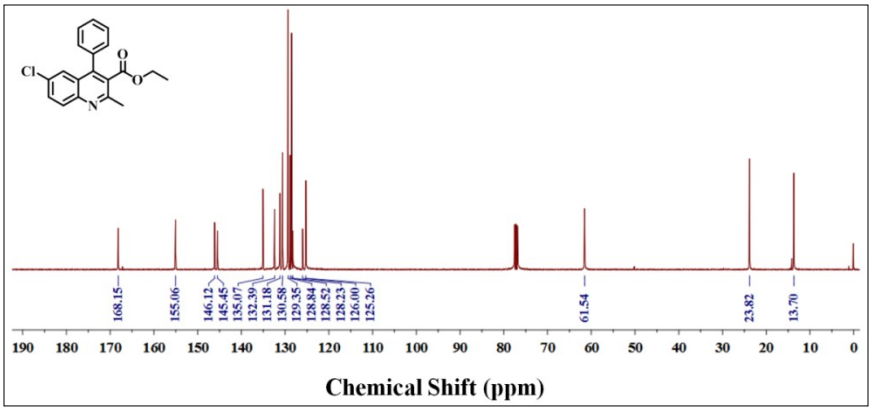

Fig. S16 ^{13}C NMR of Ethyl 6-chloro-2-methyl-4-phenylquinoline-3-carboxylate.

.

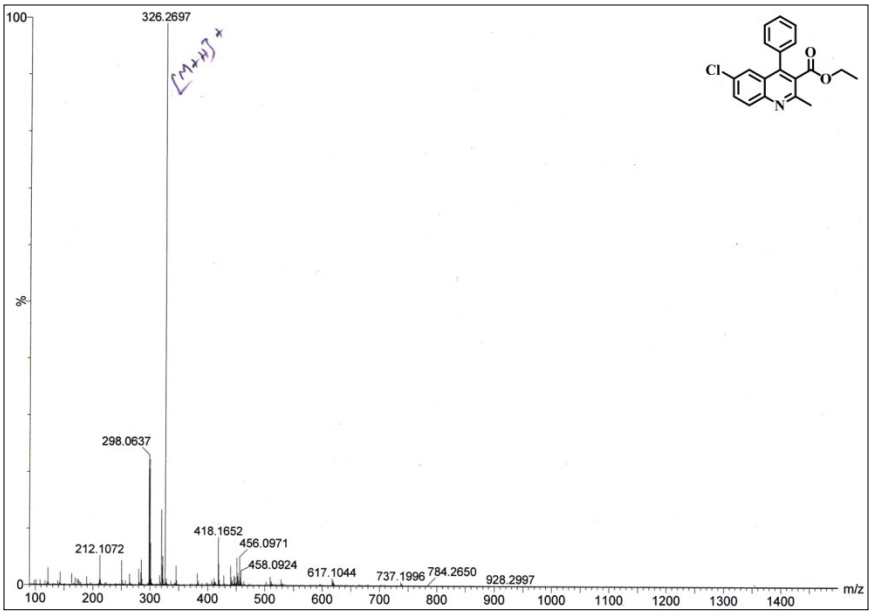

Fig. S17 ESI−MS of Ethyl 6-chloro-2-methyl-4-phenylquinoline-3-carboxylate.

Ethyl 2-methyl-6-nitro-4- phenylquinoline-3-carboxylate (Table 1, entry 3). ^{1}H NMR (400 MHz, CDCl3): δ (ppm) 8.51–8.52 (m, 1H, Ar–H), 8.45 (dd, J = 2.52 Hz, 6.68 Hz, 1H, Ar–H), 8.17 (d, J = 9.16 Hz, 1H, Ar–H), 7.51–7.54 (m, 3H, Ar–H), 7.34–7.36 (m, 2H, Ar–H), 4.07 (q, J = 7.16 Hz, 2H, –OCH_2), 2.81 (s, 3H, –CH_3), 0.95 (t, J = 7.16 Hz, 2H, –CH_3); ^{13}C NMR (100 MHz, $CDCl_3$) δ = (ppm) 13.71, 24.25, 61.87, 123.59, 123.81, 124.55, 128.83, 129.25, 129.33, 129.47, 130.84, 134.21, 145.63, 148.01, 149.78, 158.98, 167.62; MS (ESI): m/z = 337.12 $[M+H]^+$.

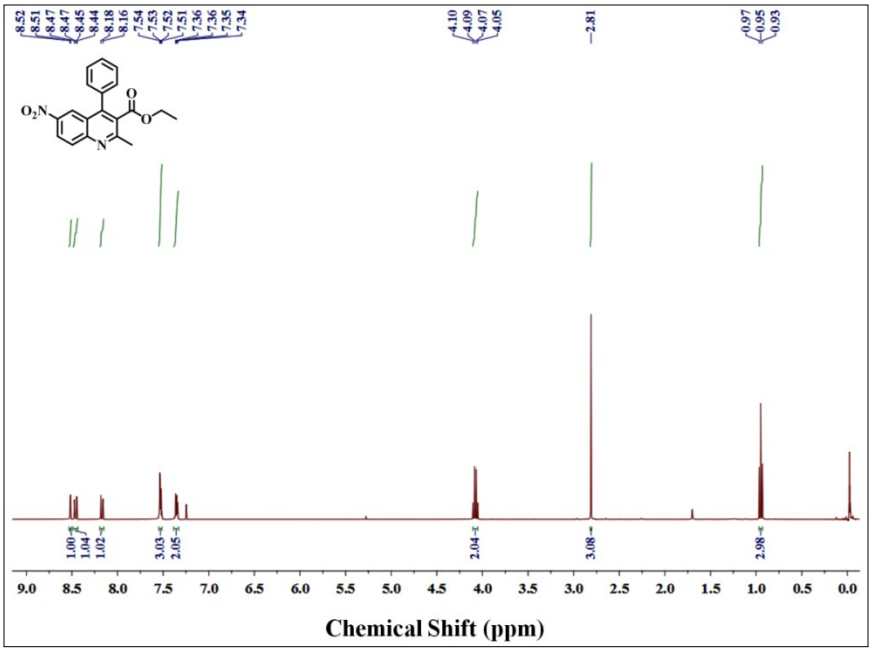

Fig. S18 ^{1}H NMR of Ethyl 2-methyl-6-nitro-4- phenylquinoline-3-carboxylate.

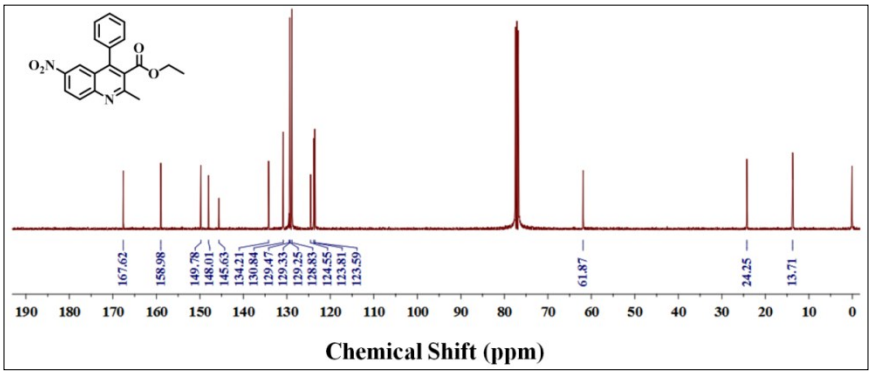

Fig. S19 ^{13}C NMR of Ethyl 2-methyl-6-nitro-4- phenylquinoline-3-carboxylate.

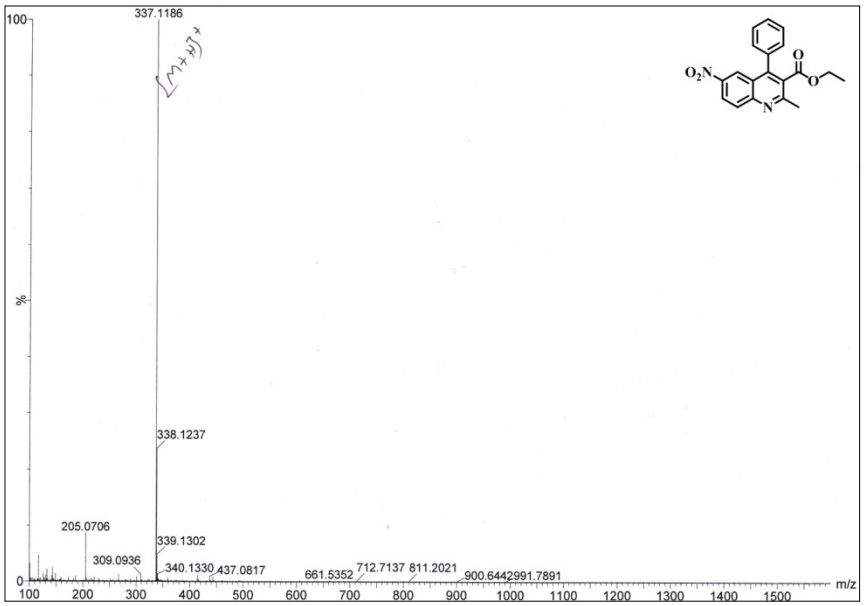

Fig. S20 ESI−MS of Ethyl 2-methyl-6-nitro-4- phenylquinoline-3-carboxylate.

1-(2-methyl-4-phenylquinolin-3-yl)ethanone (Table 1, entry 4). ^{1}H NMR (400 MHz, CDCl3): δ (ppm) 8.06 (d, J = 8.44 Hz, 1H, Ar–H), 7.71 (t, J = 8.36 Hz, 1H, Ar–H), 7.61 (d, J = 8.44 Hz, 1H, Ar–H), 7.49–7.51 (m, 3H, Ar–H), 7.43 (t, J = 7.08 Hz, 1H, Ar–H), 7.33–7.36 (m, 2H, Ar–H), 2.69 (s, 3H, –CH_3), 1.99 (s, 3H, –CH_3); ^{13}C NMR (100 MHz, $CDCl_3$) δ = (ppm) 24.00, 32.05, 125.11, 126.26, 126.62, 128.81, 128.95, 129.01, 130.12, 130.22, 134.90, 135.27, 144.02, 147.61, 153.64, 205.88; MS (ESI): m/z = 262.13 $[M+H]^+$.

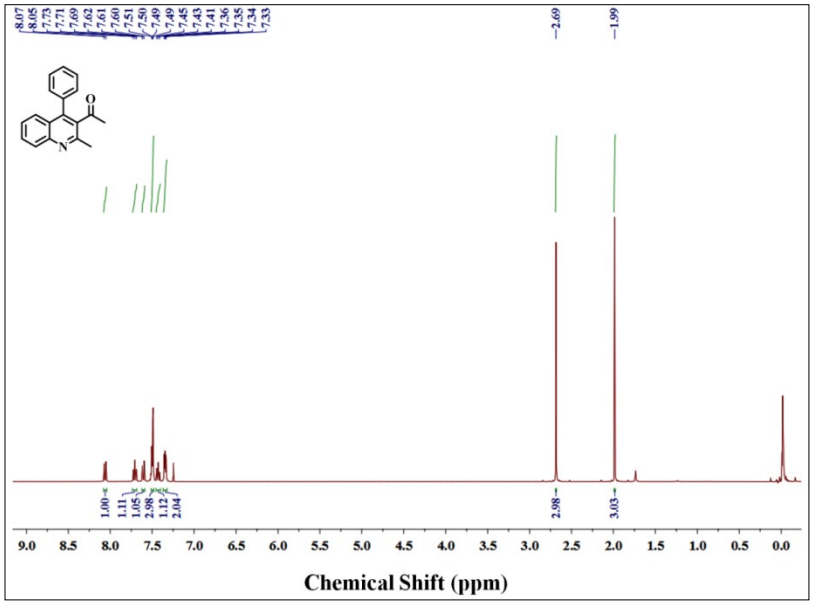

Fig. S21 ^{1}H NMR of 1-(2-methyl-4-phenylquinolin-3-yl)ethanone.

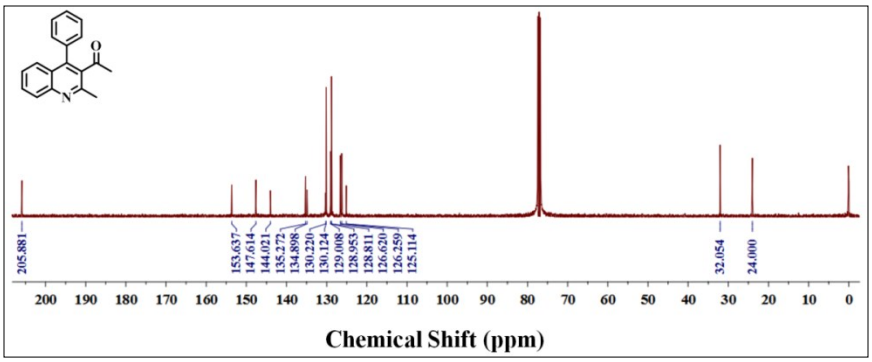

Fig. S22 ^{13}C NMR of 1-(2-methyl-4-phenylquinolin-3-yl)ethanone.

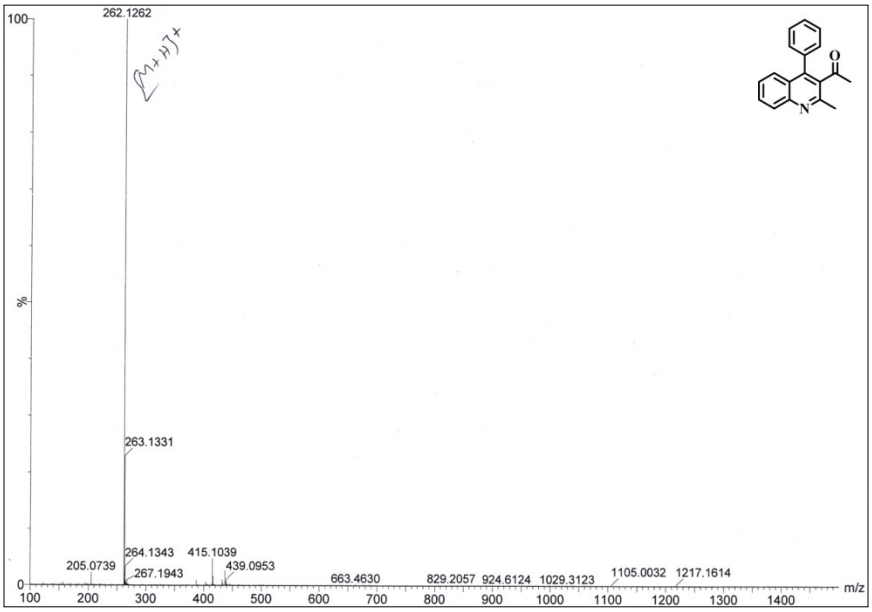

Fig. S23 ESI−MS of 1-(2-methyl-4-phenylquinolin-3-yl)ethanone.

9-phenyl-3,4-dihydroacridin-1(2*H*)-one (Table 1, entry 5). ^{1}H NMR (400 MHz, CDCl3): δ (ppm) 8.05 (d, J = 8.40 Hz, 1H, Ar–H), 7.74 (t, J = 8.32 Hz, 1H, Ar–H), 7.44–7.49 (m, 4H, Ar–H), 7.36–7.40 (m, 1H, Ar–H), 7.15–7.17 (m, 2H, Ar–H), 3.36 (t, J = 6.56 Hz, 2H, –CH_2–), 2.69 (t, J = 6.92 Hz, 2H, –CH_2–), 2.23 (quint, J = 6.64 Hz, 2H, –CH_2–); ^{13}C NMR (100 MHz, $CDCl_3$) δ = (ppm) 21.47, 34.71, 40.73, 123.93, 126.52, 127.58, 127.64, 128.10, 128.20, 128.32, 128.57, 131.84, 137.74, 148.74, 151.53, 162.34, 198.11; MS (ESI): m/z = 274.12 $[M+H]^+$.

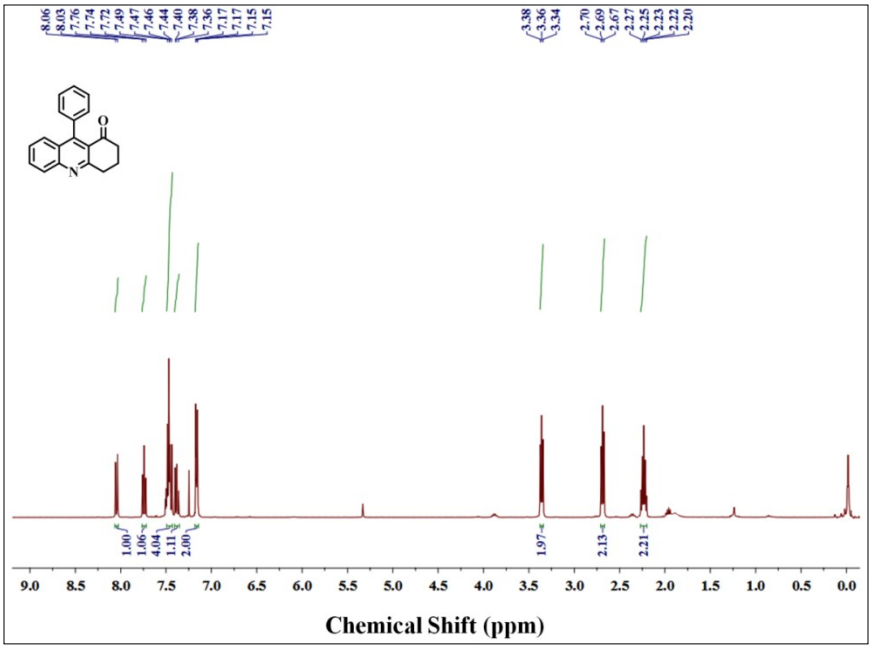

Fig. S24 ^{1}H NMR of Ethyl 2-methyl-6-nitro-4- phenylquinoline-3-carboxylate.

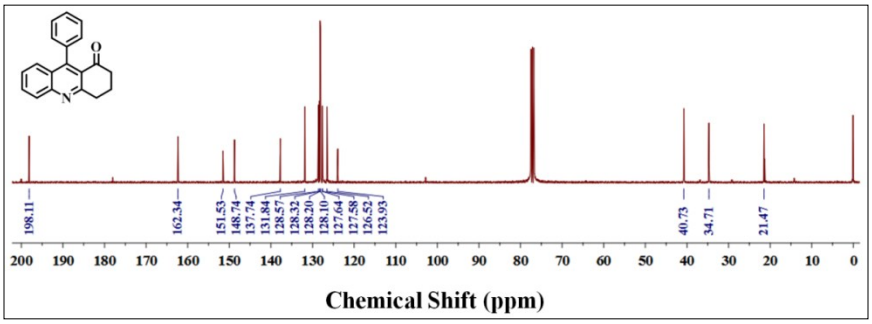

Fig. S25 ^{13}C NMR of Ethyl 2-methyl-6-nitro-4- phenylquinoline-3-carboxylate.

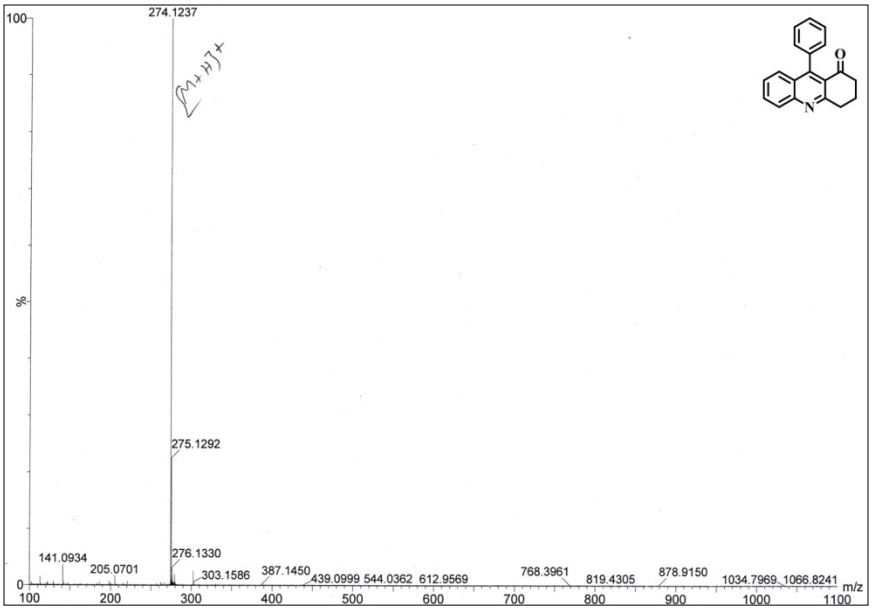

Fig. S26 ESI−MS of Ethyl 2-methyl-6-nitro-4- phenylquinoline-3-carboxylate.

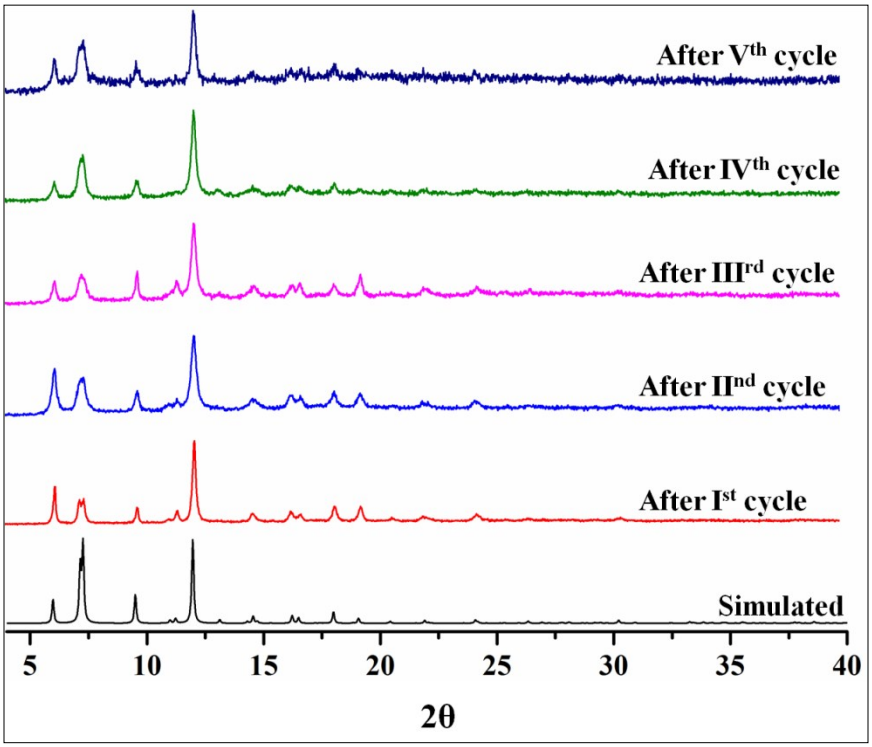

Fig. S27 Powder X-ray diffraction patterns of Simulated **1** and **1** after each catalytic cycle upto 5th cycle in the Friedländer reaction.

Compounds Characterization Data for Henry Reactions

1-(4-nitrophenyl) -2-nitroethanol (Table 2, entry 1). ^{1}H NMR (400 MHz, CDCl3): δ (ppm) 8.26 (d, J = 8.8 Hz, 2H, Ar–H), 7.61 (d, J = 8.52 Hz, 2H, Ar–H), 5.59 (dd, J = 4.04 Hz, 4.24 Hz, 1H, –CH), 4.54–4.62 (m, 2H, –CH_2–), 3.18 (bs, 1H, –OH); ^{13}C NMR (100 MHz, $CDCl_3$) δ = (ppm) 70.04, 80.68, 124.28, 124.63, 127.03, 129.87, 145.03, 148.24; MS (ESI): m/z = 211.04 $[M+H]^-$.

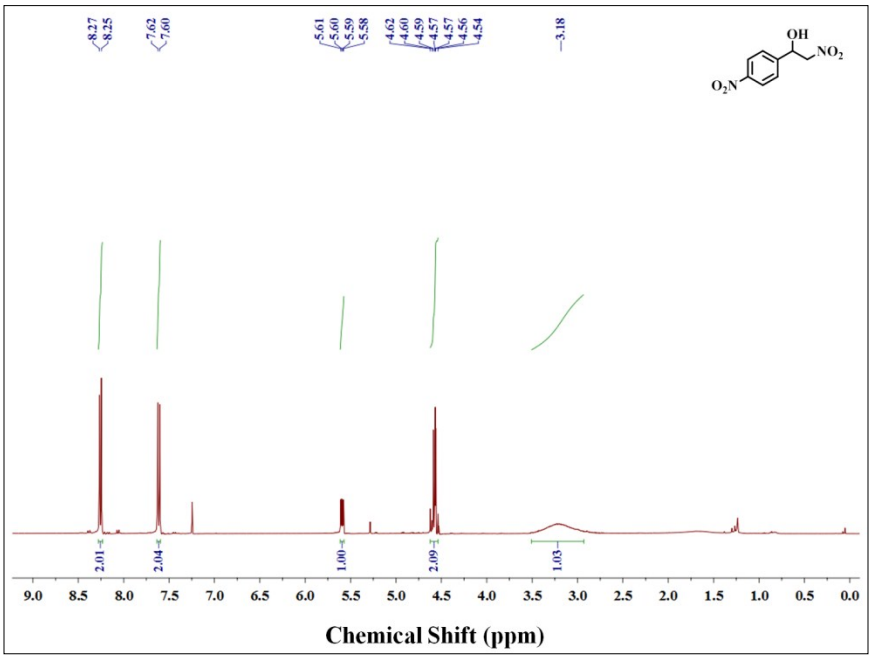

Fig. S28 ^{1}H NMR of 1-(4-nitrophenyl) -2-nitroethanol.

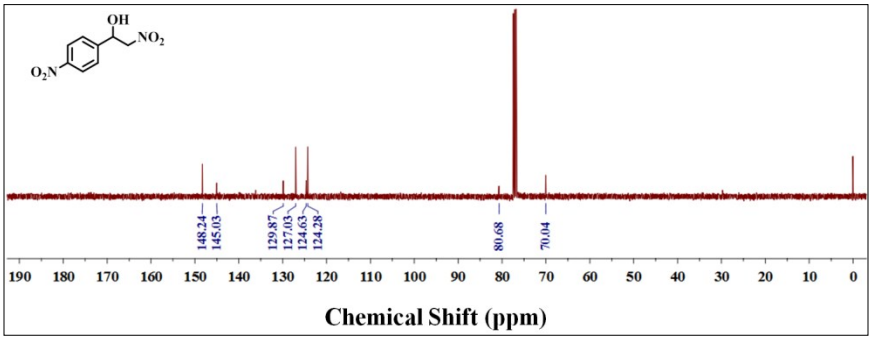

Fig. S29 ^{13}C NMR of 1-(4-nitrophenyl) -2-nitroethanol.

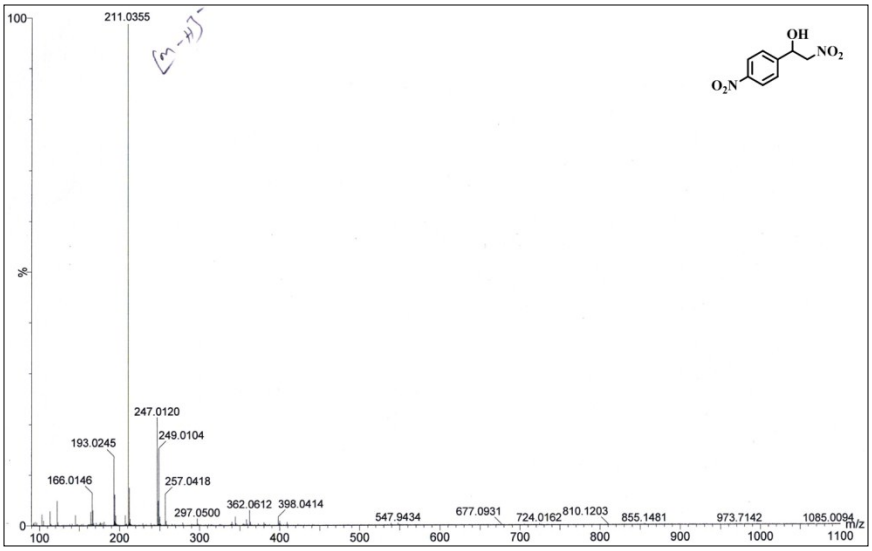

Fig. S30 ESI−MS of 1-(4-nitrophenyl) -2-nitroethanol.

1-(2-nitrophenyl)-2-nitroethanol (Table 2, entry 2). ^{1}H NMR (400 MHz, CDCl3): δ (ppm) 8.07 (d, J = 6.92 Hz, 1H, Ar–H), 7.94 (d, J = 7.88 Hz, 1H, Ar–H), 7.74 (t, J = 7.6 Hz, 1H, Ar–H), 7.52–7.56 (m, 1H, Ar–H), 6.05 (dd, J = 2.16 Hz, 6.96 Hz, 1H, –CH), 4.85–4.89 (m, 1H, –CH_2–), 4.52–4.58 (m, 1H, –CH_2–), 3.15 (bs, 1H, –OH); ^{13}C NMR (100 MHz, $CDCl_3$) δ = (ppm) 66.85, 80.13, 125.11, 128.71, 129.78, 134.07, 134.48, 147.26; MS (ESI): m/z = 211.04 $[M+H]^-$.

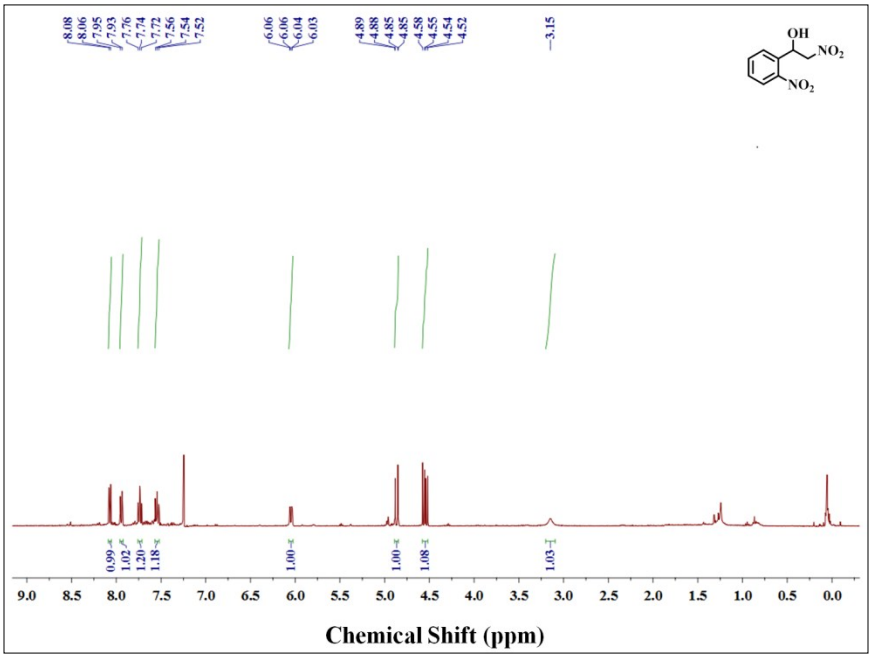

Fig. S31 ^{1}H NMR of 1-(2-nitrophenyl)-2-nitroethanol.

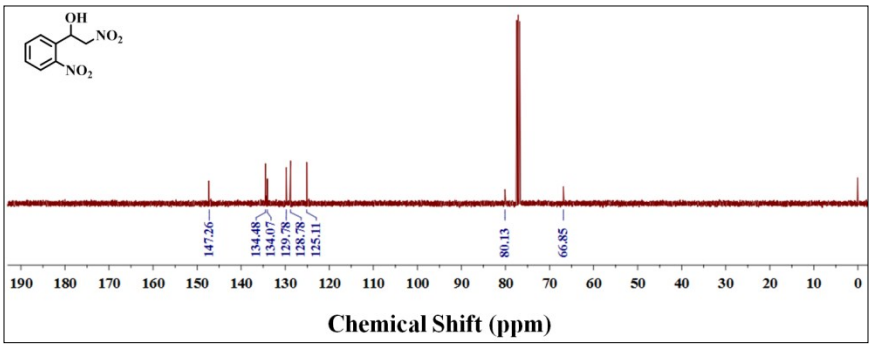

Fig. S32 ^{13}C NMR of 1-(2-nitrophenyl)-2-nitroethanol.

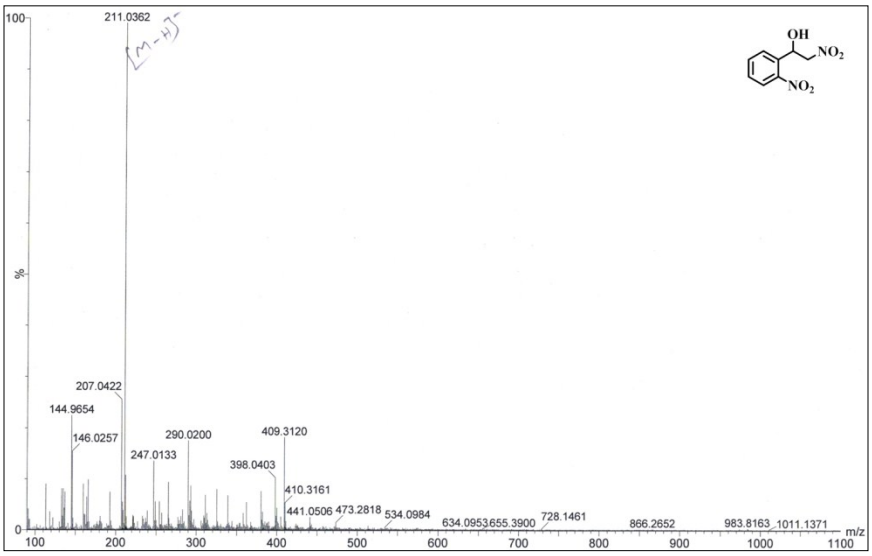

Fig. S33 ESI−MS of 1-(2-nitrophenyl)-2-nitroethanol.

1-(3-nitrophenyl)-2-nitroethanol (Table 2, entry 3). ^{1}H NMR (400 MHz, CDCl3): δ (ppm) 8.28 (s, 1H, Ar–H), 8.17 (d, J = 7.16 Hz, 1H, Ar–H), 7.75 (dd, J = 1.72 Hz, 7.76 Hz, 1H, Ar–H), 7.59 (t, J = 8 Hz, 1H, Ar–H), 5.59 (dd, J = 3.72 Hz, 4.24 Hz, 1H, –CH), 4.57–4.65 (m, 2H, –CH_2–), 3.42 (s, 1H, –OH); ^{13}C NMR (100 MHz, $CDCl_3$) δ = (ppm) 69.93, 80.78, 121.23, 123.87, 130.22, 132.21, 140.41, 148.55; MS (ESI): m/z = 211.04 $[M+H]^-$.

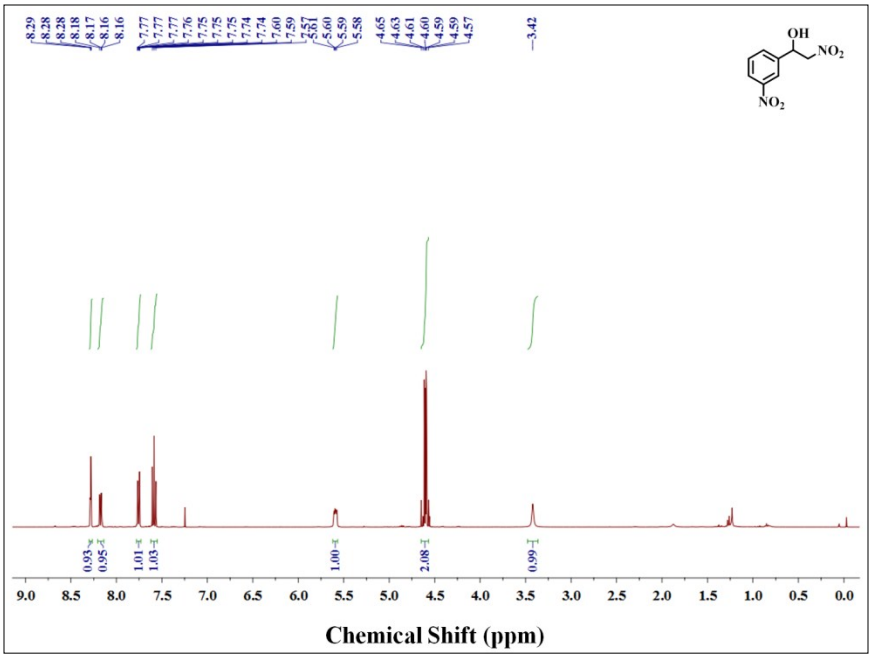

Fig. S34 ^{1}H NMR of 1-(3-nitrophenyl)-2-nitroethanol.

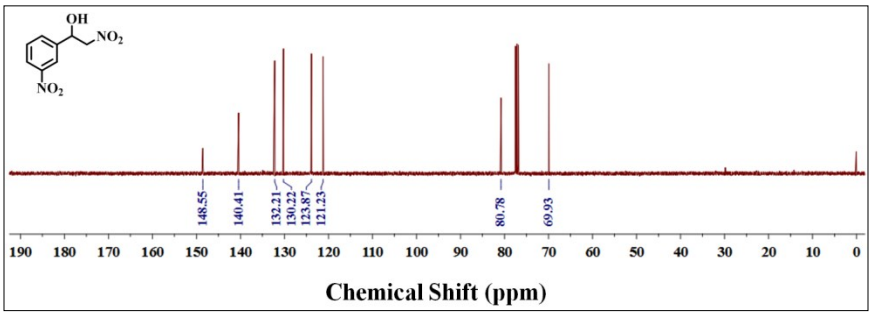

Fig. S35 ^{13}C NMR of 1-(3-nitrophenyl)-2-nitroethanol.

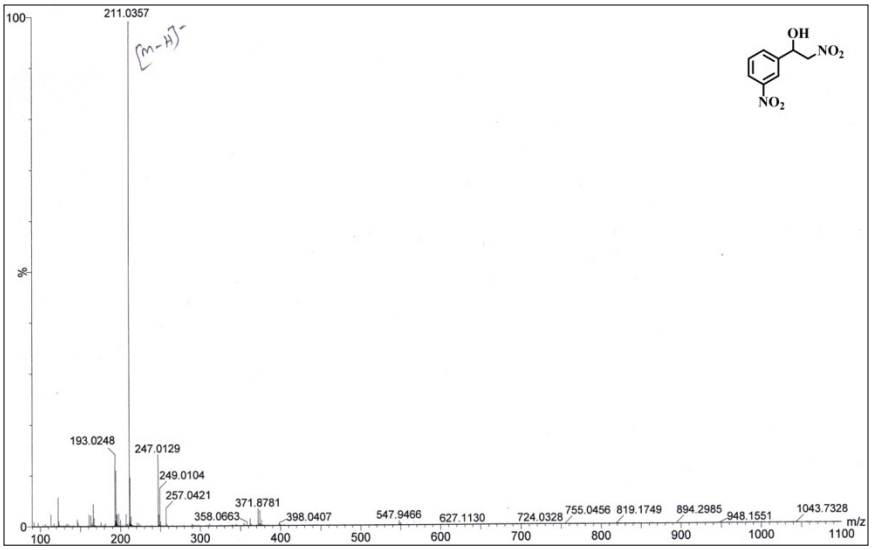

Fig. S36 ESI−MS of 1-(3-nitrophenyl)-2-nitroethanol.

1-phenyl-2-nitroethanol (Table 2, entry 4). ^{1}H NMR (400 MHz, CDCl3): δ (ppm) 7.33–7.41 (m, 5H, Ar–H), 5.46 (dd, J = 3.04 Hz, 6.56 Hz, 1H, –CH), 4.49–4.63 (m, 2H, –CH_2–), 2.80 (bs, 1H, –OH); ^{13}C NMR (100 MHz, $CDCl_3$) δ = (ppm) 71.09, 81.03, 126.01, 127.24, 129.14, 138.15; MS (ESI): m/z = 166.04 $[M+H]^-$.

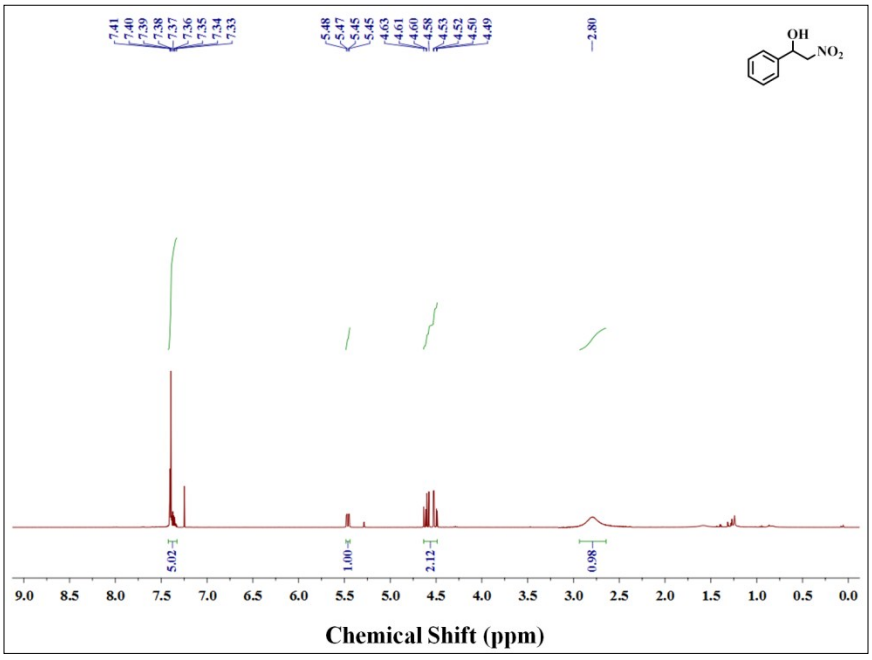

Fig. S37 ^{1}H NMR of 1-phenyl-2-nitroethanol.

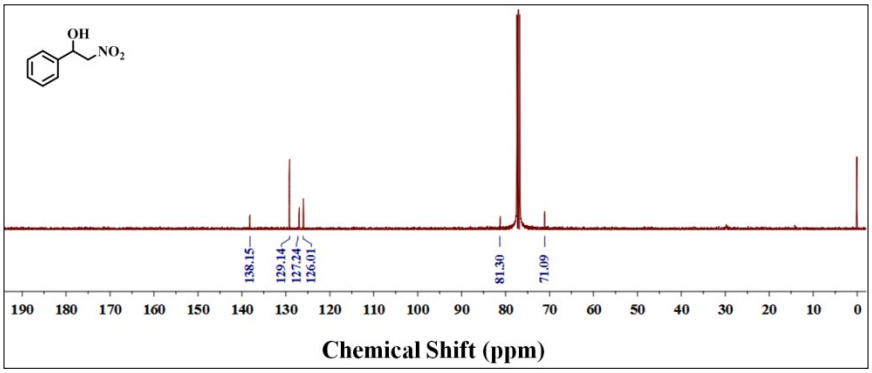

Fig. S38 ^{13}C NMR of 1-phenyl-2-nitroethanol.

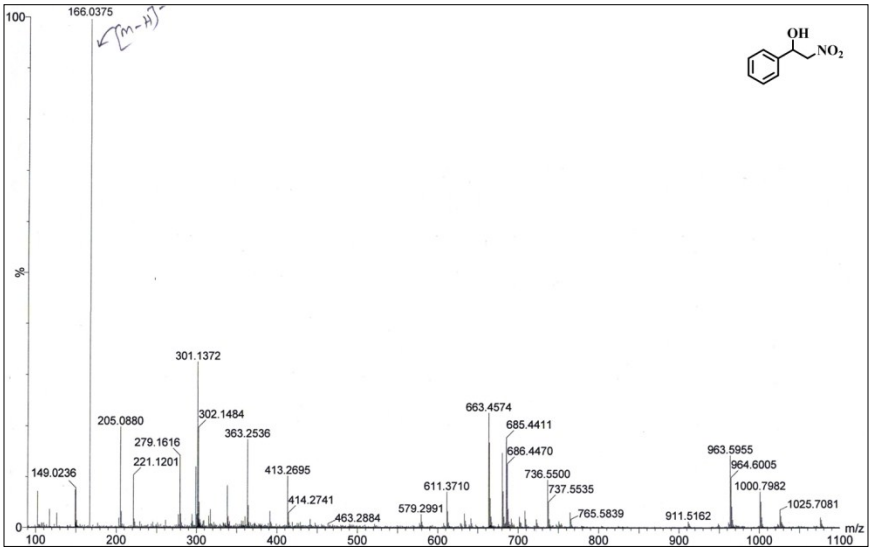

Fig. S39 ESI−MS of 1-phenyl-2-nitroethanol.

1-(4-methylphenyl) -2-nitroethanol (Table 2, entry 5). ^{1}H NMR (400 MHz, CDCl3): δ (ppm) 7.28 (d, J = 8.12 Hz, 2H, Ar–H), 7.20 (d, J = 7.96 Hz, 2H, Ar–H), 5.42 (dd, J = 3 Hz, 6.56 Hz, 1H, –CH), 4.46–4.62 (m, 2H, –CH_2–), 2.87 (bs, 1H, –OH), 2.35 (s, 3H); ^{13}C NMR (100 MHz, $CDCl_3$) δ = (ppm) 21.84, 70.83, 88.52, 126.90, 129.78, 135.41, 139.27; MS (ESI): m/z = 180.90 $[M+H]^-$.

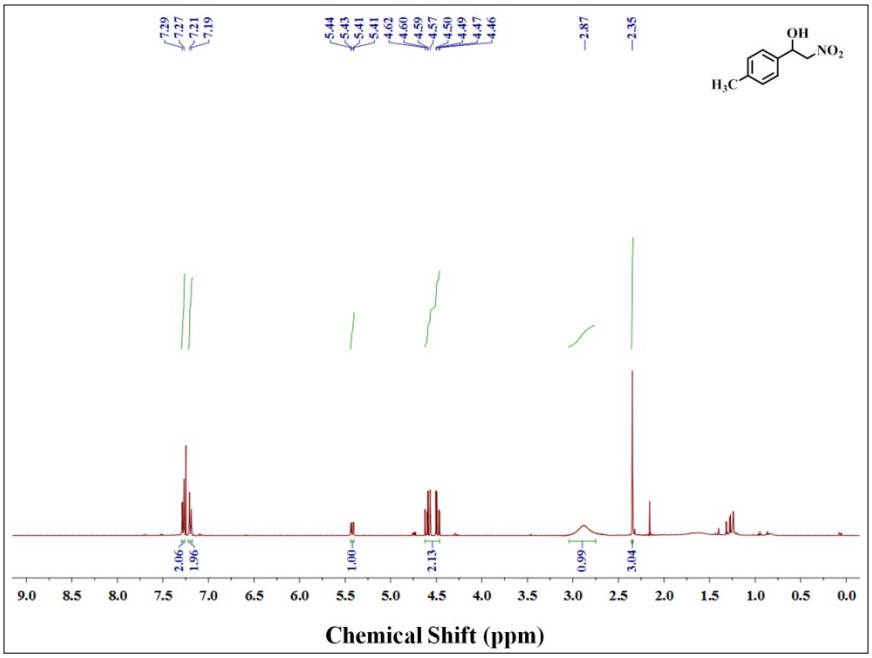

Fig. S40 ^{1}H NMR of 1-(4-methylphenyl) -2-nitroethanol.

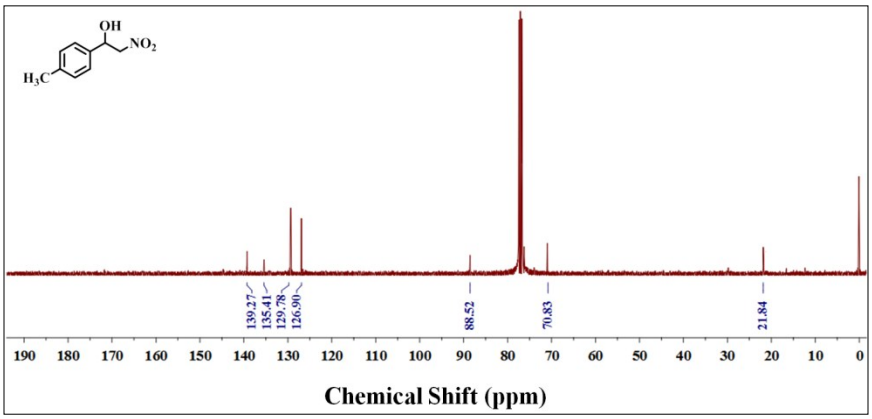

Fig. S41 ^{13}C NMR of 1-(4-methylphenyl) -2-nitroethanol.

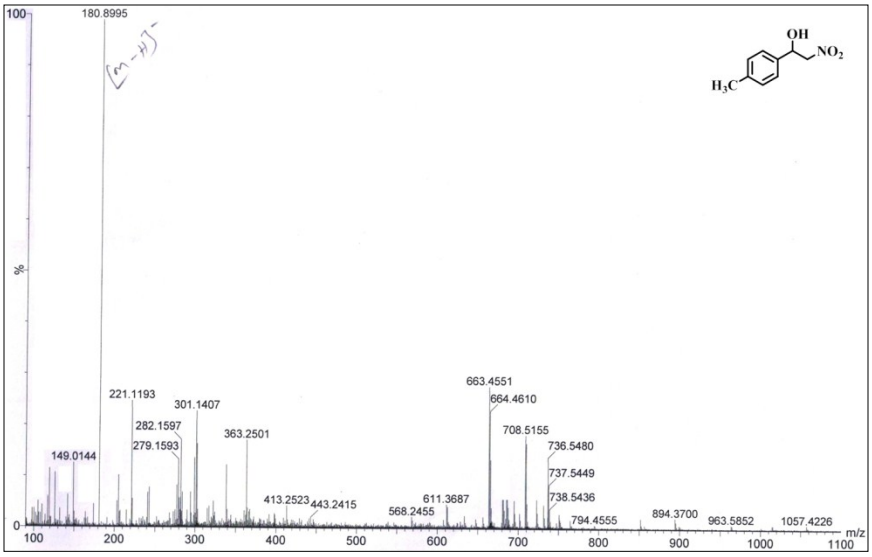

Fig. S42 ESI−MS of 1-(4-methylphenyl) -2-nitroethanol.

1-(4-fluorophenyl)-2-nitroethanol (Table 2, entry 6). ^{1}H NMR (400 MHz, CDCl3): δ (ppm) 7.38 (dd, J = 3.64 Hz, 5.24 Hz, 2H, Ar–H), 7.08 (t, J = 8.52 Hz, 2H, Ar–H), 5.44 (dd, J = 3.04 Hz, 6.4 Hz, 1H, –CH), 4.46–4.60 (m, 2H, –CH_2–), 2.85 (bs, 1H, –OH); ^{13}C NMR (100 MHz, $CDCl_3$) δ = (ppm) 70.41, 116.77, 127.90, 131.32, 137.93, 165.13; MS (ESI): m/z = 184.04 $[M+H]^-$.

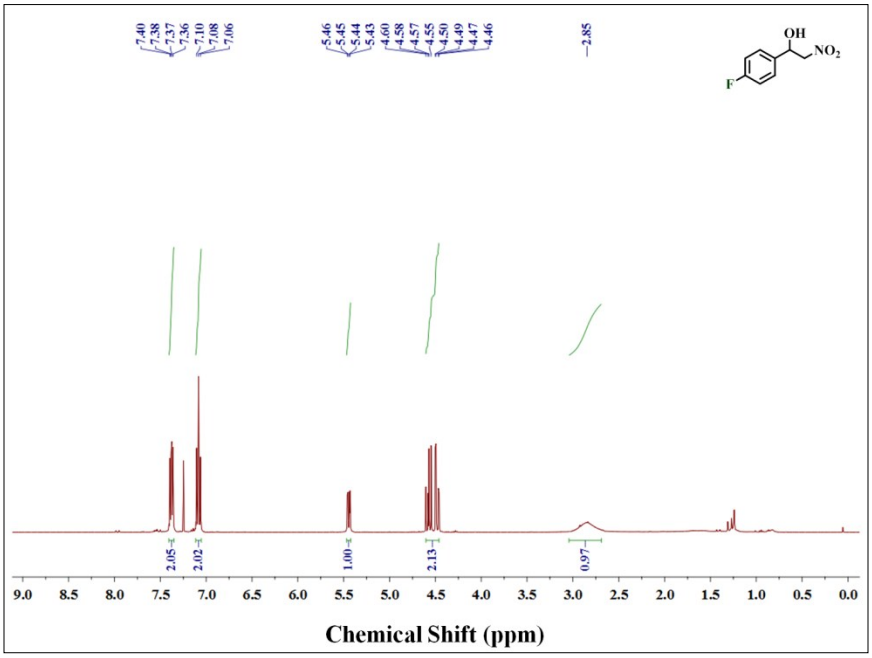

Fig. S43 ^{1}H NMR of 1-(4-fluorophenyl)-2-nitroethanol.

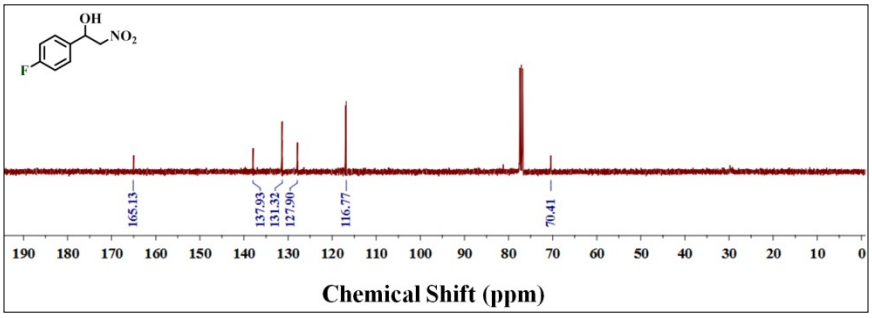

Fig. S44 ^{13}C NMR of 1-(4-fluorophenyl)-2-nitroethanol.

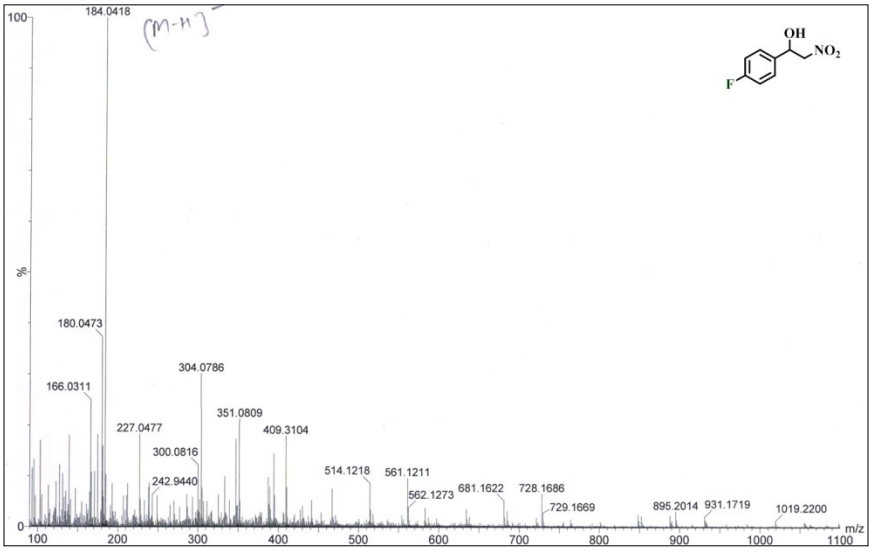

Fig. S45 ESI−MS of 1-(4-fluorophenyl)-2-nitroethanol.

1-(4-nitrophenyl)-2-nitropropan-1-ol (Table 2, entry 7). Diastereomeric ratio (*syn*/*anti* 67:33) determined by 1H NMR; *Syn* isomer: ^{1}H NMR (400 MHz, CDCl3): δ (ppm) 8.21–8.24 (m, 2H, Ar–H), 7.55–7.59 (m, 2H, Ar–H), 5.17 (d, J = 8.36 Hz, 1H, –CH), 4.68–4.79 (m, 1H, –CH), 3.09 (bs, 1H, –OH), 1.36 (d, J = 6.88 Hz, 3H, CH3). *Anti* isomer: ^{1}H NMR (400 MHz, CDCl3): δ (ppm) 8.21–8.24 (m, 2H, HAr Ar–H), 7.55–7.59 (m, 2H, Ar–H), 5.54 (m, 1H, –CH), 4.68–4.79 (m, 1H, –CH), 3.09 (bs, 1H, –OH), 1.46 (d, J = 6.84 Hz, 3H, CH3).

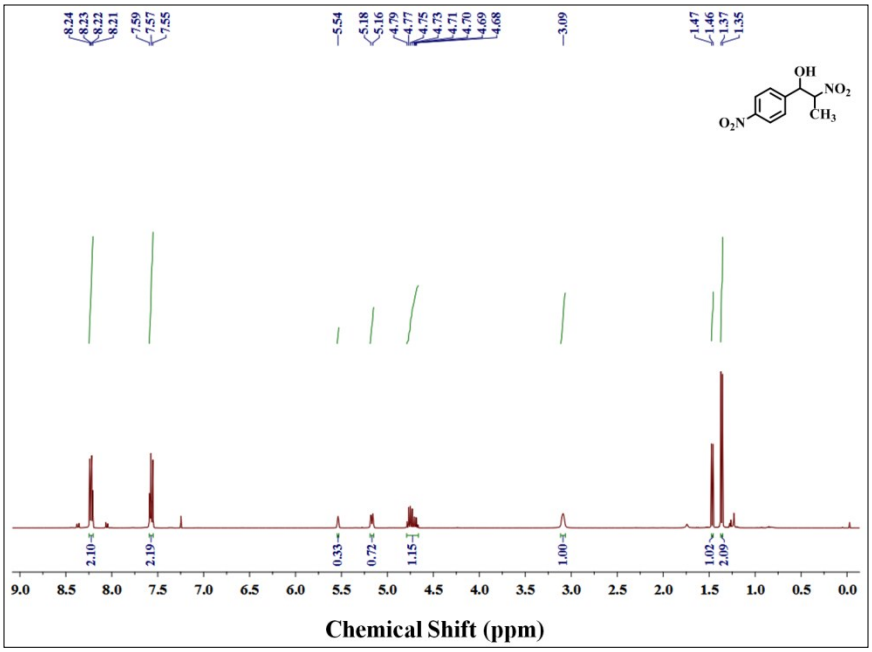

Fig. S46 ^{1}H NMR of 1-(4-nitrophenyl)-2-nitropropan-1-ol.

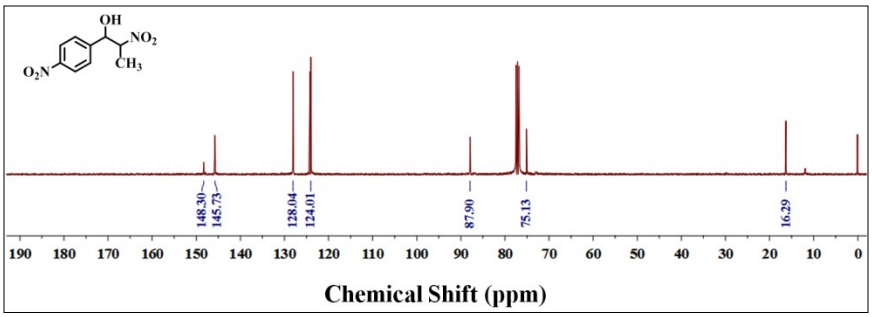

Fig. S47 ^{13}C NMR of 1-(4-nitrophenyl)-2-nitropropan-1-ol.

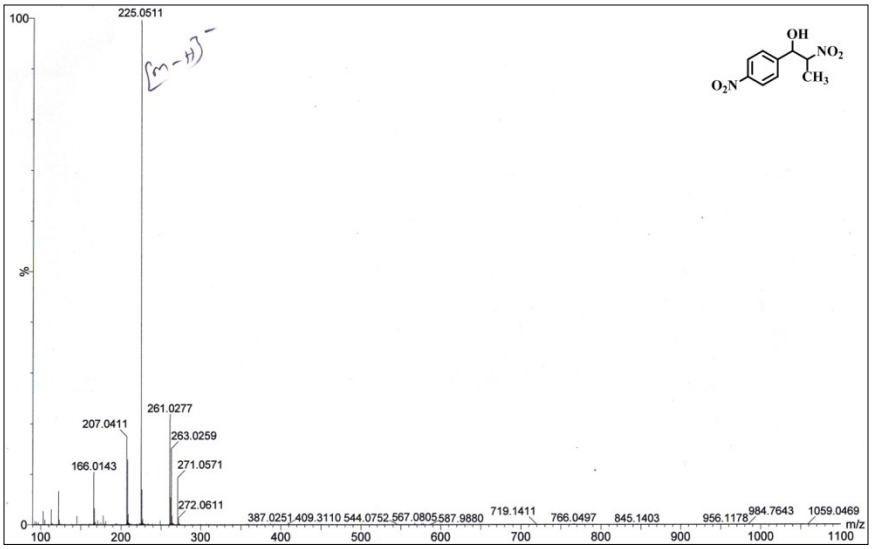

Fig. S48 ESI−MS of 1-(4-nitrophenyl)-2-nitropropan-1-ol.

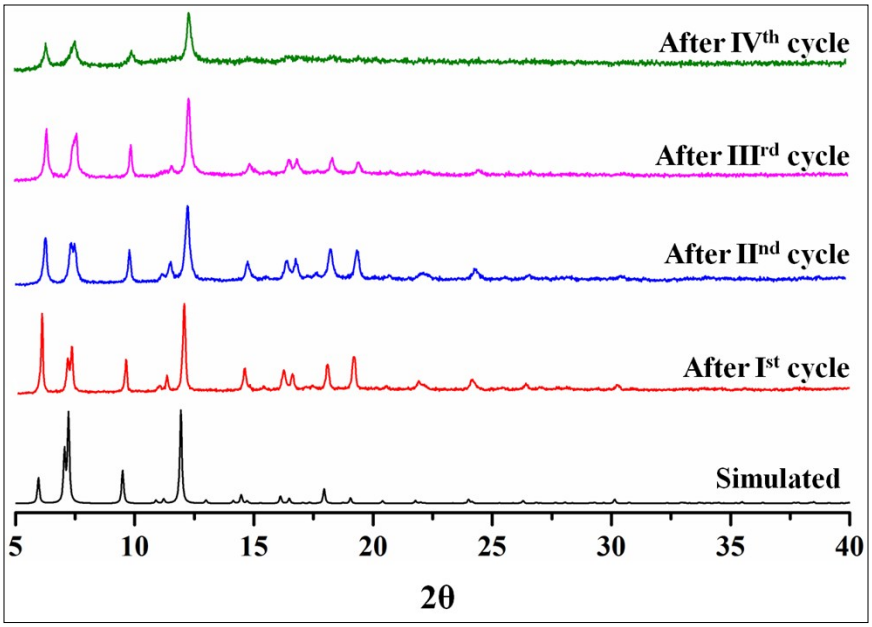

Fig. S49 Powder X-ray diffraction patterns of **1** and **1** after each catalytic cycle upto 4th cycle in the Henry reactions.

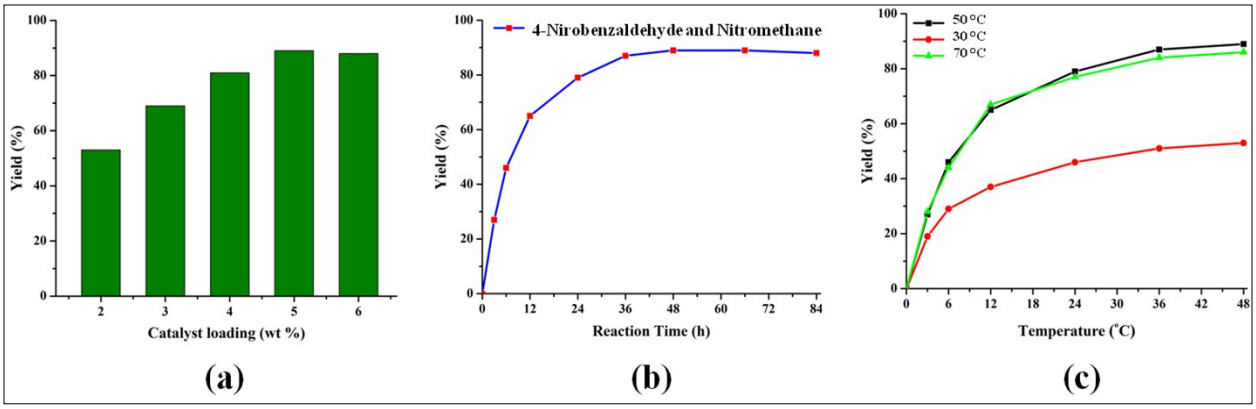

Fig. S50 Showing the optimized catalyst loading in wt % (a), reaction time in h (b), and reaction temperature in ºC (c).

References

(1) Q. Mu, H. Wang, L. Li, C. Wang, Y. Wang and X. Zhao, *Chem. —Asian J.*, 2015, **10**, 1864–1869.

(2) L. Osorio-Planes, C. Rodríguez-Escrich, and M. A. Pericàs, *Org. Lett.*, 2014, **16**, 1704−1707.

(3) SMART & SAINT Software Reference Manuals, version 6.45; Bruker Analytical X-ray Systems, Inc.:Madison, WI, **2003**.

(4) Sheldrick, G. M. *SADABS* a software for empirical absorption correction; version 2.05; Program for Empirical Absorption Correction of Area Detector Data. University of Göttingen: Göttingen, Germany, **2002**.

(5) (a) SHELXTL Reference Manual, version 6.1; Bruker Analytical Xray Systems, Inc.: Madison, WI, **2000**. (b) Sheldrick, G. M. SHELXTL v.6.12, Bruker AXS Inc., Madison, WI, **2001**.

(6) Sheldrick, G. M. A short history of SHELX. Acta Crystallogr., Sect. A: Found. Crystallogr. **2008**, *64*, 112–122.

(7) Dolomanov, O.V.; Bourhis, L.J.; Gildea, R.J.; Howard, J.A.K.; Puschmann, H., Olex2: A complete structure solution, refinement and analysis program. *J. Appl. Cryst*. **2009**, *42*, 339-341.

(8) Spek, A. L. PLATON, A Multipurpose Crystallographic Tool. The University of Utrecht: Utrecht, The Netherlands, **2013**.